Imatinib triggers mesenchymal-like conversion of CML cells associated with increased aggressiveness

Alexandre Puissant, Maeva Dufies, Nina Fenouille, Issam Ben Sahra, Arnaud Jacquel, Guillaume Robert, Thomas Cluzeau, Marcel Deckert, Mélanie Tichet, Yann Chéli, et al.

doi:10.1093/jmcb/mjs010
Published online March 31, 2012

Article

Imatinib triggers mesenchymal-like conversion of CML cells associated with increased aggressiveness

Alexandre Puissant[1,2,3,4], Maeva Dufies[1,2,3], Nina Fenouille[2,5,6], Issam Ben Sahra[2,7,8], Arnaud Jacquel[1,2,3], Guillaume Robert[1,2,3], Thomas Cluzeau[1,2,3,9], Marcel Deckert[2], Mélanie Tichet[2,5], Yann Chéli[2,5], Jill-Patrice Cassuto[1,10], Sophie Raynaud[9], Laurence Legros[9], Jean-Max Pasquet[11], François-Xavier Mahon[11], Frédéric Luciano[1,2,3], and Patrick Auberger[1,2,3,*]

[1] INSERM U1065, Team: Cell Death, Differentiation, Inflammation and Cancer, Nice, France
[2] Université de Nice, Sophia Antipolis, Nice, France
[3] Equipe labellisée par la Ligue Nationale Contre le Cancer (2011–2013), Paris, France
[4] Present address: Dana-Farber Cancer Institute, Boston, MA, USA
[5] INSERM U1065, Team: Biology and Pathology of Melanocytic Cells, Nice, France
[6] Present address: Massassuchetts Institute of Technology (MIT), Boston, MA, USA
[7] INSERM U1065, Team: Cellular and Molecular Physiopathology of Obesity, Nice, France
[8] Present address: Harvard School of Public Health, Boston, MA, USA
[9] Service d'Onco-hématologie, CHU, Nice, France
[10] Service d'Hématologie Clinique et de Transplantation, CHU, Nice, France
[11] INSERM U1035, Hématologie leucémique et cibles thérapeutiques, Bordeaux, France
* Correspondence to: Patrick Auberger, INSERM U1065, 151 Route de Saint-Antoine de Ginestière, BP 2 3194, 06204 Nice Cedex 3, France.
E-mail: auberger@unice.fr

Chronic myelogenous leukemia (CML) is a cytogenetic disorder resulting from the expression of p210BCR-ABL. Imatinib, an inhibitor of BCR-ABL, has emerged as the leading compound to treat CML patients. Despite encouraging clinical results, resistance to imatinib represents a major drawback for therapy, as a substantial proportion of patients are refractory to this treatment. Recent publications have described the existence of a small cancer cell population with the potential to exhibit the phenotypic switch responsible for chemoresistance. To investigate the existence of such a chemoresistant cellular subpopulation in CML, we used a two-step approach of pulse and continuous selection by imatinib in different CML cell lines that allowed the emergence of a subpopulation of adherent cells (IM-R Adh) displaying an epithelial–mesenchymal transition (EMT)-like phenotype. Overexpression of several EMT markers was observed in this CML subpopulation, as well as in $CD34^+$ CML primary cells from patients who responded poorly to imatinib treatment. In response to imatinib, this $CD44^{high}/CD24^{low}$ IM-R Adh subpopulation exhibited increased adhesion, transmigration and invasion *in vitro* and *in vivo* through specific overexpression of the $\alpha V\beta 3$ receptor. FAK/Akt pathway activation following integrin β3 (ITGβ3) engagement mediated the migration and invasion of IM-R Adh cells, whereas persistent activation of ERK counteracted BCR-ABL inhibition by imatinib, promoting cell adhesion-mediated resistance.

Keywords: chronic myelogenous leukemia, $CD44^{high}/CD24^{low}$ subpopulation, cell adhesion-mediated drug resistance (CAM-DR), imatinib resistance, ITGB3

Introduction

Chronic myelogenous leukemia (CML) is a hematopoietic stem cell disease characterized by t(9;22)(q34;q11) translocation, which encodes the chimeric tyrosine kinase p210BCR-ABL (Groffen et al., 1984). This tyrosine kinase is responsible for the increased activation of several downstream signaling pathways, including the Ras/Raf/MEK/ERK and PI3K/Akt pathways, which both affect malignant cell behavior (Deininger et al., 2000; Steelman et al., 2004).

The tyrosine kinase inhibitor (TKI) imatinib is the first-line treatment option for patients with CML; however, prolonged drug exposure may result in the acquisition of drug resistance, impeding successful treatment, and causing patient relapse (Druker et al., 2001; O'Brien et al., 2003). Many studies have been conducted without considering CML as a homeostatic disease of the bone marrow (BM) that is not limited to the leukemic population but extends to the surrounding medullar stroma. To date, it is incompletely understood how BCR-ABL and TKIs (including imatinib) affect the tumor–stroma interactions in the BM to create a permissive and supporting microenvironment for malignancy and for the dissemination of leukemic stem cells.

Received August 5, 2011. Revised February 2, 2012. Accepted February 22, 2012.

In a physiological context, interactions with the medullar stroma control the homeostasis of normal hematopoietic stem cells in the adapted microenvironment of the BM (Hope and Bhatia, 2011). The proliferation of normal hematopoietic progenitors is significantly inhibited when these cells are cultured in contact with BM stromal cells or with the adhesive matrix protein fibronectin (FN), suggesting that integrin-dependent adhesion inhibits normal progenitor cell proliferation (Hurley et al., 1995; Salesse and Verfaillie, 2002). In contrast, the abnormal expansion of CML progenitors and their growth advantages over existing normal progenitors may be related to their inability to integrate and transduce negative signals from the BM microenvironment (Salesse and Verfaillie, 2002). Thus, decreased integrin-mediated adhesion of CML progenitors to the medullar stroma may underlie the expansion of malignant CML progenitors and their evasion from the BM (Shet et al., 2002). In addition, the BM microenvironment can efficiently protect leukemic cells against apoptosis induced by cytotoxic drugs, TKIs and γ-irradiation. Indeed, CML cells in contact with stromal cells and extracellular matrix components may acquire resistance to chemotherapy (Damiano et al., 1999, 2001) by a process known as cell adhesion-mediated drug resistance (CAM-DR) (Li and Dalton, 2006). Although it is well established that CML cell progenitors in the BM are less sensitive to imatinib than their circulating counterparts, the role of cell adhesion in the resistance of CML cell progenitors to TKIs has not been evaluated (Li and Dalton, 2006).

Emerging lines of evidence suggest that the acquisition of drug resistance reflects changes in cell–cell and cell–matrix communication of the tumor cells, which can undergo a transdifferentiation process such as epithelial-to-mesenchymal transition (EMT; Thiery, 2002; Voulgari and Pintzas, 2009). EMT is a highly conserved developmental program allowing epithelial cells to transdifferentiate into cells displaying a mesenchymal phenotype (Thiery et al., 2009). This program is activated during mesoderm formation and speciation of hematopoietic progenitors in embryos; however, it also promotes the metastatic dissemination of single malignant cells following the acquisition of adhesive, migratory and invasive capacities (Thiery et al., 2009). Recent evidence that induction of the mesenchymal phenotypic switch generates chemorefractory cells with stem cell-like features emphasized the role of EMT in tumorigenesis (Mani et al., 2008; Ahmed et al., 2010; Mego et al., 2010; Wang et al., 2011).

In the present study, we demonstrate that continuous imatinib treatment selects for a subpopulation of imatinib-resistant and highly adherent CML cells (IM-R Adh) that expressed stemness markers and exhibited mesenchymal behavior compared with their imatinib-sensitive (IM-S) counterparts. The spreading phenotype of IM-R Adh cells is associated with increased invasive properties that strictly depend on the presence of imatinib or nilotinib in the culture medium as it was rapidly reversible upon drug withdrawal. The increased adhesion, migration and invasive properties of IM-R Adh cells *in vitro* and *in vivo* are mediated specifically through enhanced αVβ3 integrin expression and signaling that culminate in the activation of the FAK/Akt and ERK1/2 pathways. Of note, overexpression of the β3 integrin is also observed in primary mononuclear cells from CML patients treated for 1 year with imatinib. Collectively, these findings show for the first time that continuous incubation of IM-R CML cells with TKIs (imatinib or nilotinib) selects for adherent cells with a cancer-initiating cell and EMT-like phenotype that have acquired an increased capacity for adhesion, migration and invasion *in vitro* and *in vivo*.

Results

Phenotypic and functional characterization of imatinib-dependent adherent CML cells

From the IM-S K562 and JURL-MK1 CML cell lines, we generated CML cell lines resistant to imatinib (IM-R) following pulse exposure to increasing doses of imatinib. As a first step, IM-S cells were treated with 0.1 μM imatinib for 5 days and were then washed and maintained in culture for two additional days in the absence of imatinib. Then, increasing concentrations of imatinib (2.5-fold increments) were sequentially administered up to 10 μM. Subsequently, IM-R cells were grown continuously in the presence of imatinib to mimic the daily, long-term exposure to TKIs of CML patients. Under these conditions, we observed the rapid emergence of a small proportion of cells with a spread morphology. After several cycles of replating in the continuous presence of high doses of imatinib, we isolated a new subpopulation of K562 or JURL-MK1 adherent cells, hereafter referred to as K562 and JURL-MK1 IM-R Adh cells (Figure 1A, left panel). As shown by phalloidin staining, imatinib increased the adherence and spreading of this new subpopulation of IM-R Adh cells by inducing a reorganization of the actin cytoskeleton network (Figure 1A, right panel). Because imatinib selected for a new cell population with increased adhesive properties, we investigated whether these cells were capable of forming 3D spheroids, which is a hallmark of cancer-initiating cells. As shown in Figure 1B, only IM-R Adh but not IM-S cells were capable of forming 3D spheroids in 24-well plates coated with soft agar, suggesting that these cells display cancer stem cell-like phenotypic characteristics and behavior. A possible explanation for this phenotype is an enrichment of the IM-R Adh cell subpopulation with leukemia-initiating cells (LIC). To compare the frequency of LIC in the IM-S and IM-R Adh cell populations, we performed a limiting dilution assay using standard methods (Hu and Smyth, 2009). The average LIC frequency in the IM-R Adh cell population increased 11-fold compared with IM-S cells (1/3430 versus 1/39210; Figure 1C). Accordingly, IM-R Adh cells were homogeneously $CD34^{med}/CD38^{low}$ (Figure 1D), a phenotype associated with leukemic stem cell potential. Although slightly slower growing than IM-S cells as a result of the high proportion of cells in the G0/G1 phase of the cell cycle (Supplementary Figure S1A and B), IM-R Adh cells were proliferative, as shown by the Ki-67 staining in Figure 1E. Moreover, imatinib treatment did not impair the capacity of IM-R Adh cells to proliferate, in contrast to IM-S cells (Supplementary Figure S1B). Finally, both K562 cell types exhibited an equivalent mitochondrial membrane potential that remains unchanged after imatinib treatment of IM-R Adh cells (Supplementary Figure S1C). As observed in Supplementary Figure S1D and E, imatinib-induced caspase 9 and 3 activation that correlated with a decrease in Bcl-2 protein levels in IM-S cells, while the Bcl-2 expression was sustained despite imatinib treatment in IM-R Adh cells.

To further characterize the stem cell-like phenotype of the IM-R Adh cell subpopulation, we screened several known markers of

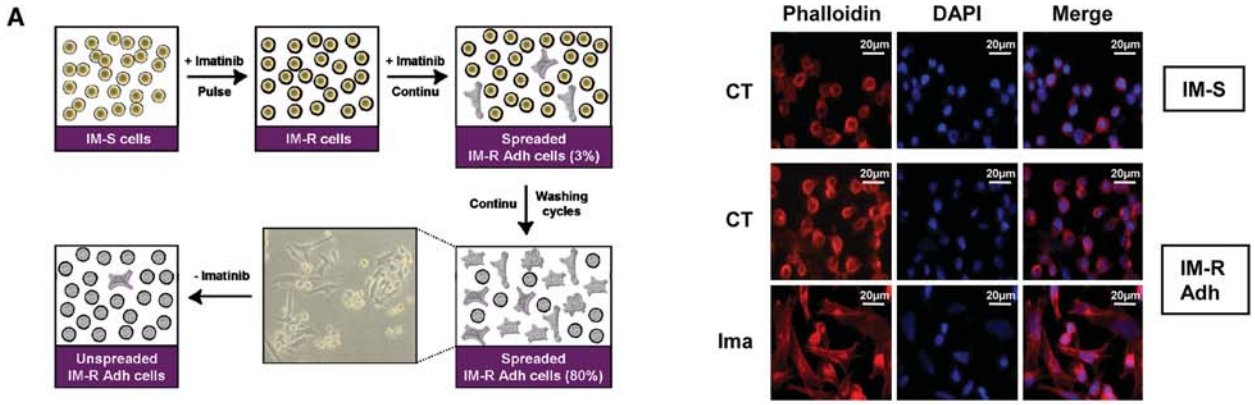

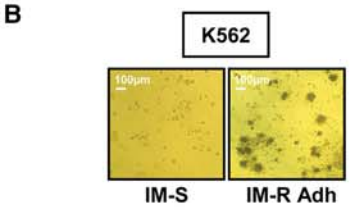

C

	Number of tumors / Number of injected mice					Leukemia-initiating cell frequency (95% confidence interval)	Increase
IM-S	6/6	5/6	3/7	0/5	0/6	1/39210 (1/16340 – 1/94100)	
IM-R Adh	6/6	6/6	5/7	4/5	2/6	1/3430 (1/1400– 1/8360)	x 11.4
Cells per injection	1 000 000	100 000	10 000	1 000	100		

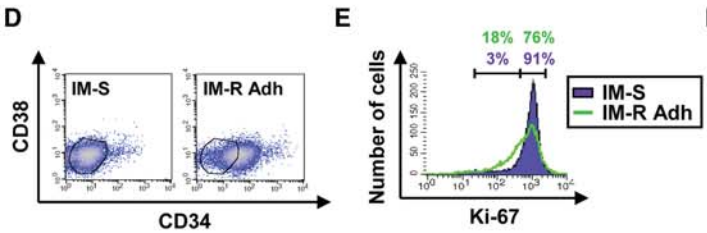

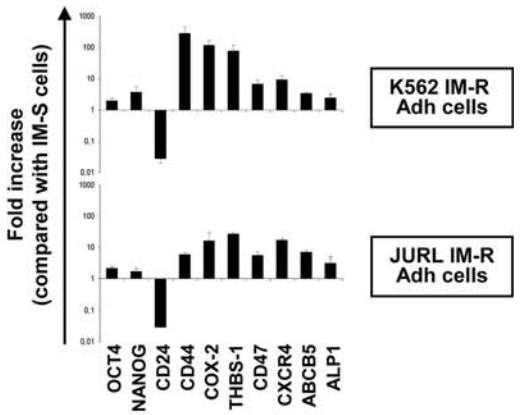

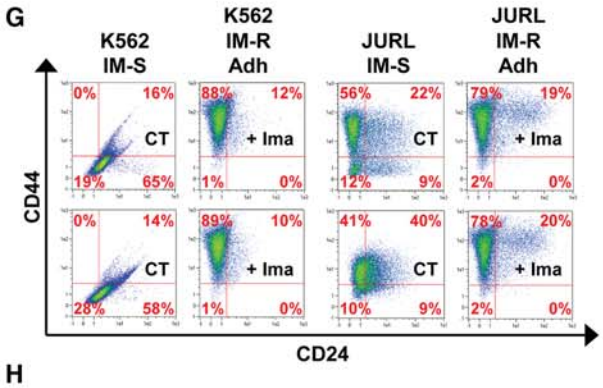

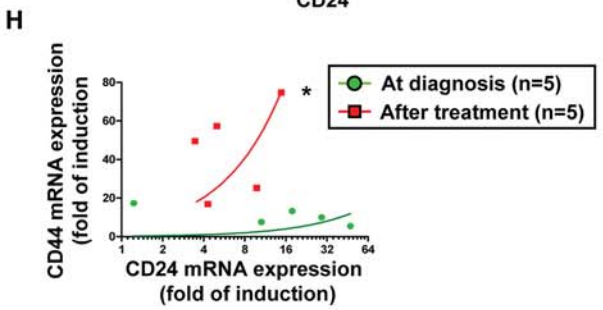

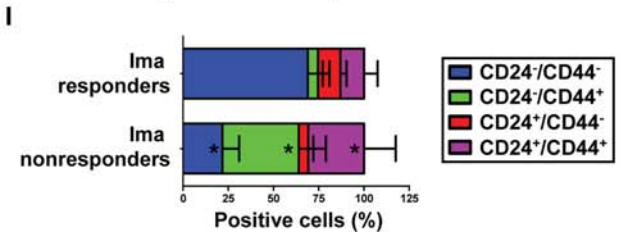

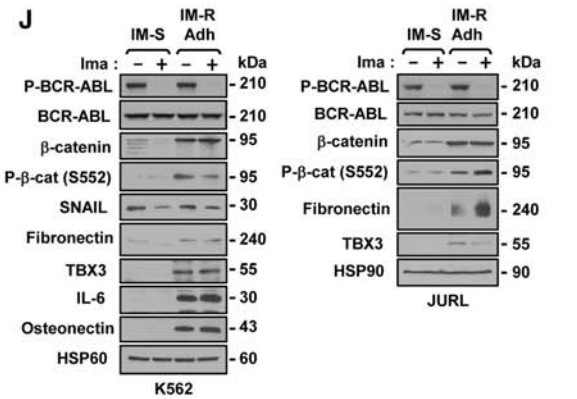

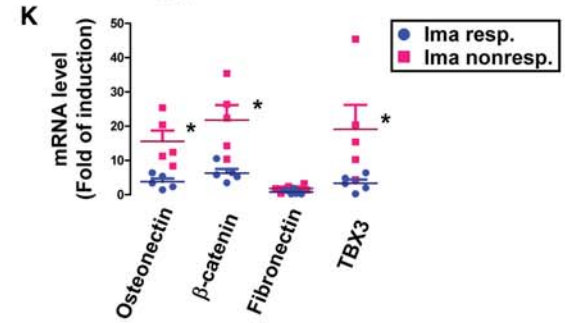

cancer stem cells by quantitative PCR (qPCR) microplates. Significant increases in the expression of stemness markers including Oct4, Nanog and ALP1 were observed in two different IM-R-Adh CML cell lines (K562 and JURL-MK1) compared with their IM-S counterparts (Figure 1F). Importantly, these cells also exhibit an additional stem cell-like signature that is characterized by both a drastic upregulation of CD44 and a downregulation of CD24. CD24 and CD44 are both cell-surface glycoproteins involved in cell–cell interactions, cell adhesion and migration. Although CD44 is expressed in a large number of mammalian cell types and participates in a wide variety of cellular functions including lymphocyte activation, recirculation and homing and hematopoiesis, CD24 expression is restricted to most B lymphocytes and differentiating neuroblasts (Gires, 2011). The first description of a $CD44^{high}/CD24^{low}$ population with stem/progenitor cell properties was reported in breast cancer (Sheridan et al., 2006; Kai et al., 2010). This $CD44^{high}/CD24^{low}$ population of breast cancer-initiating cells displayed the aggressive traits of cells that have undergone the EMT (Mani et al., 2008). EMT programs, normally silenced after embryonic development, are reactivated by $CD44^{high}/CD24^{low}$ cells to acquire a mesenchymal phenotype responsible for spreading, colonization/homing and proliferation at sites of metastasis. Enhanced expression of CXCR4 and COX-2, other markers associated with the $CD44^{high}/CD24^{low}$ population, was also observed in K562 and JURL-MK1 IM-R Adh cells (Figure 1F). Moreover, THBS-1 and its receptor CD47, which participate in cell adhesion, migration and homing, was significantly upregulated in these adherent cells. We next used flow cytometry analysis to confirm the $CD44^{high}/CD24^{low}$ expression pattern. Although most IM-S K562 cells were $CD44^{low}/CD24^{high}$, imatinib allowed the emergence of a large majority (90%) of $CD44^{high}/CD24^{low}$ IM-R Adh K562 cells, which reflects precisely the phenotype that has been ascribed to neoplastic mammary stem cells undergoing an EMT program (Figure 1G). Interestingly, a significant proportion of JURL-MK1 IM-S cells already expressed CD44 and CD24 markers, whereas a majority (80%) of JURL-MK1 IM-R cells were CD44 positive and CD24 negative. To expand these findings to a clinical level, we performed qPCR analysis of CD24 and CD44 markers on peripheral blood mononuclear cells (PBMCs) from 5 CML patients newly diagnosed with CML or in partial cytogenetic response after a 1-year treatment with imatinib (Figure 1H). Importantly, each patient at diagnosis had a very low expression level of CD44 mRNA and a high expression level of CD24 mRNA (green dots), while the opposite pattern of CD24 and CD44 mRNA expression was observed in imatinib-treated patients (red square). To confirm these results, we analyzed by flow cytometry a second set of CML $CD34^{+}$ cells from imatinib-responder patients with a complete cytogenetic response within 1 year and imatinib-non-responder patients lacking a major cytogenetic response after 1 year (Figure 1I). Imatinib-non-responder CML cells showed a higher proportion of $CD44^{high}$ cells than imatinib-responder cells that were essentially $CD24^{low}/CD44^{low}$.

Finally, the mesenchymal-like phenotype of both CML IM-R Adh cell lines was confirmed by constitutive activation of the β-catenin network resulting from a sustained level of phospho-β-catenin (S552) (which is a central EMT signaling pathway) and increased expression of mesenchymal markers such as the matricial proteins osteonectin and FN. However, vimentin remained undetectable in all CML cell lines (not shown). As shown in Supplementary Figure S2, both IM-S and IM-R Adh K562 IM-R cells secreted FN into the culture medium, and imatinib (as expected) decreased FN secretion only by IM-S cells. The expression level of the transcription factor TBX3, which controls the EMT program, was also up-regulated (Figure 1J). In agreement with these results, the mRNA expression of osteonectin, β-catenin and TBX3, but not FN, was also increased in imatinib-non-responder-primary cells (Figure 1K). However, the expression of SNAIL, an EMT master regulator, was found to be identical in IM-S and IM-R Adh cells (Figure 1J). Finally, BCR-ABL was completely dephosphorylated following imatinib treatment of K562 and JURL-MK1 IM-R Adh cells, ruling out the possibility that ABL domain point mutations are responsible for the resistance of these cells to imatinib. This observation was confirmed through sequencing of the ABL domain of BCR-ABL (data not shown).

Imatinib promotes the adhesion and transmigration of IM-R Adh cells and their invasiveness in vitro and in vivo

We next evaluated the adhesion, migration and invasion properties associated with the EMT stem cell-like phenotype of the

Figure 1 Imatinib allows the expansion of a cell subpopulation that has stemness properties and expresses EMT-initiating cell markers. (**A**) Imatinib allows the expansion of a small population of adherent and spread CML cells (IM-R Adh cells) (left panel); and IM-S and IM-R Adh K562 CML cells were treated with 3 μM imatinib or vehicle control for 8 h, fixed, stained with 2.5 μg/ml phalloidin (red) with 1 mg/ml DAPI (blue), and analyzed by epifluorescence microscopy (right panel). (**B**) Analysis of the capacity of IM-R Adh and IM-S K562 cells to form spheroids was performed as described in Materials and methods. (**C**) An *in vivo* limiting dilution assay was performed to identify the enrichment of LIC in the K562 IM-R Adh cell subpopulation. (**D** and **E**) After staining for both CD34 and CD38 (**D**) or Ki-67 (**E**), K562 IM-S and IM-R Adh cells were analyzed by flow cytometry. (**F**) Quantitative PCR analysis of the indicated invasion or stem cell markers was performed in IM-S and IM-R Adh cell lines. The results represent the ratio (fold induction ± SD) of mRNA expression in IM-R Adh cells (K562 and JURL MK1) versus their IM-S counterparts and are the mean of three independent experiments. mRNA expression levels under each condition were normalized to GAPDH levels. (**G**) K562 or JURL-MK1 IM-S and IM-R Adh cells were treated with 3 μM imatinib for 48 h. The proportion of $CD24^{high}/CD44^{low}$ and $CD24^{low}/CD44^{high}$ cells was assessed by FACS analysis. (**H**) Q-PCR analysis of CD24 and CD44 markers was performed on CML cells from five patients at diagnosis (green line) or in partial cytogenetic response after 1 year of therapy with imatinib (red line). (**I**) The proportion of the CD24/CD44 subpopulation of $CD34^{+}$ CML cells from imatinib-responder ($n = 6$) and non-responder patients ($n = 5$) was quantified by flow cytometry. (**J**) K562 or JURL-MK1 IM-S and IM-R Adh cells were treated for 8 h with 3 μM imatinib. After treatment, phospho-BCR-ABL (Y245 of ABL), phospho-β-catenin (S552), BCR-ABL, β-catenin, SNAIL, fibronectin, TBX3, IL-6, osteonectin and HSP60/90 (loading control) protein levels were visualized by immunoblotting. (**K**) Q-PCR analysis of mesenchymal markers was performed on $CD34^{+}$ CML cells from five imatinib-responder (blue dots) or non-responder (pink squares) patients. (**H**, **I**, and **K**) $*P < 0.05$ was considered significant.

subpopulation of CML IM-R Adh cells. In the absence of imatinib, K562 and JURL-MK1 IM-R Adh CML cells adhered at a basal level (15%–20%) to an FN matrix. This basal level of adhesion was also observed when imatinib-non-responder CD34$^+$ primary cells were seeded on an FN matrix (Figure 2B). To determine if increased basal adhesion occurred predominantly in imatinib-non-responder primary cells harboring a point mutation in BCR-ABL, we directly compared the basal adhesion capability of BCR-ABL WT and mutated CML cells (Supplementary Figure S3A). Interestingly, we found no difference in adhesion between these two subtypes of resistant cells. To strengthen these results, we transduced IM-R Adh cells with two known BCR-ABL mutants (T315 and M351T) frequently found in resistant patients and found no impairment of their adhesion properties (Supplementary Figure S3B).

In the presence of increasing concentrations of imatinib, more than 80% of K562 IM-R cells and 60% of JURL-MK1 IM-R CML cells adhered tightly to the FN substratum after 6 h (Figure 2A). Increased adhesion was detected 5 min following imatinib addition and was maximal at ~2 h (Figure 2C). Interestingly, 5 min after imatinib was removed from the culture medium, IM-R cell adhesiveness and spreading decreased and returned to basal levels at 8 h (Figure 2D). In addition to imatinib, nilotinib also increased the adhesion of IM-R Adh cells. In contrast, neither PD166326 (a dasatinib analog that is a dual BCR-ABL and src kinase inhibitor) nor sunitinib (Figure 2E and F), two TKIs with different mechanisms of action from the former two drugs, modulated the adhesive properties of the K562 and JURL-MK1 IM-R Adh cell populations.

In addition to the acquisition of new imatinib-dependent adhesive properties, IM-R Adh K562 and JURL-MK1 cells exhibited an increased ability to spread and transmigrate across a TNFα-stimulated HUVEC primary endothelial cell monolayer following imatinib treatment (Figure 3A and Supplementary Figure S4). To assess their transmigratory potential *in vivo*, red-labeled IM-S and green-labeled IM-R Adh CML cells were injected in equal

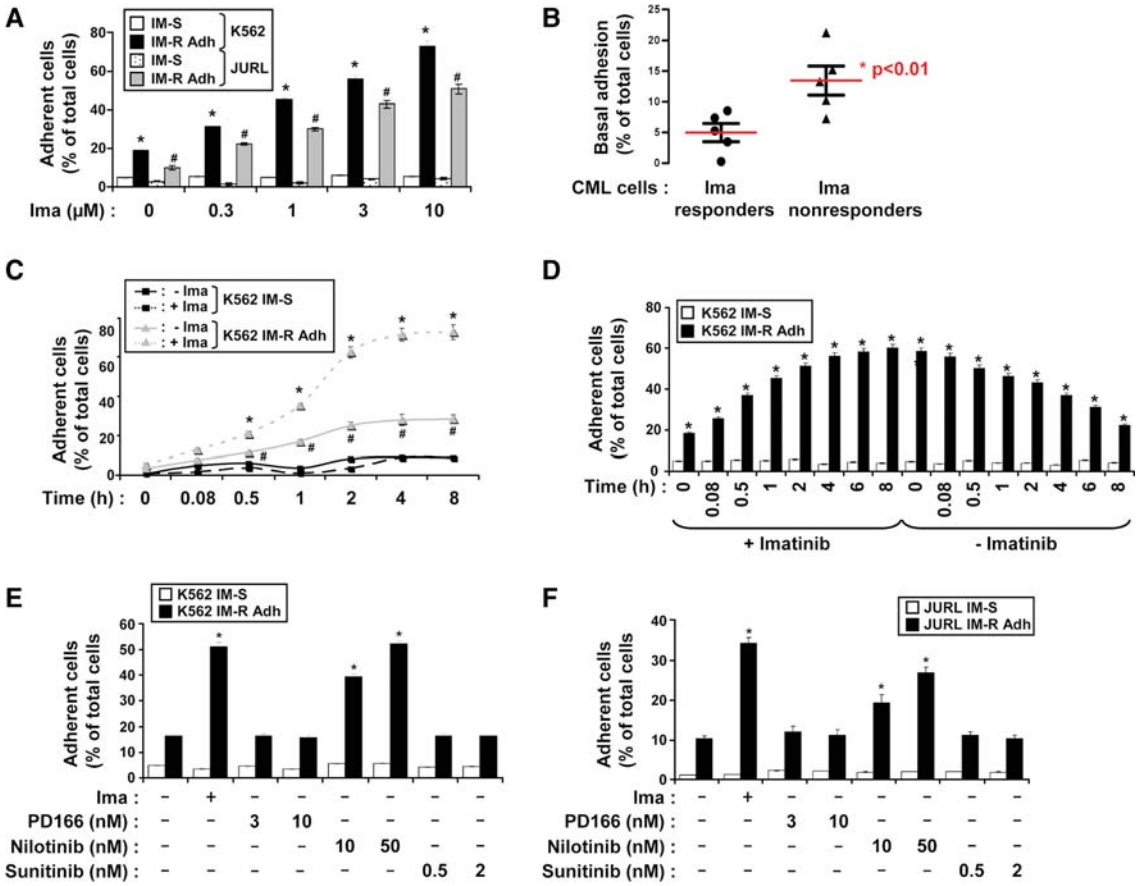

Figure 2 The IM-R Adh cell subpopulation exhibits novel high basal adhesion properties that are enhanced by TKI treatment. (**A** and **B**) IM-S and IM-R Adh cell lines (**A**) and CD34$^+$ primary cells from five imatinib-responder or non-responder patients (**B**) were stained with 2 μM CellTracker green probe, plated on 96-well plates and stimulated with increasing concentrations of imatinib for 8 h. The number of adherent cells was determined following excitation at 390 nm. (**C**) K562 IM-S and IM-R Adh cells were treated with 3 μM imatinib for various times. For each time, the number of adherent cells was determined as previously described. (**D**) The adhesion of K562 IM-S and IM-R Adh cells treated for various time with 3 μM imatinib was measured as described in **A**. In the same experiment, de-adhesion of these cells following imatinib removal was observed in the same time frame. (**E** and **F**) K562 (**E**), JURL-MK1 (**F**) IM-S and IM-R Adh CML cells were stimulated for 8 h with various concentrations of imatinib, nilotinib, PD166326, or sunitinib. The number of adhesive cells was assessed as described previously. The results in **A**–**F** are expressed as the percentage of adherent cells versus total cells and represent the mean ± SD of four independent experiments performed in quadruplicate. $^{\#,*}P < 0.05$ was considered significant.

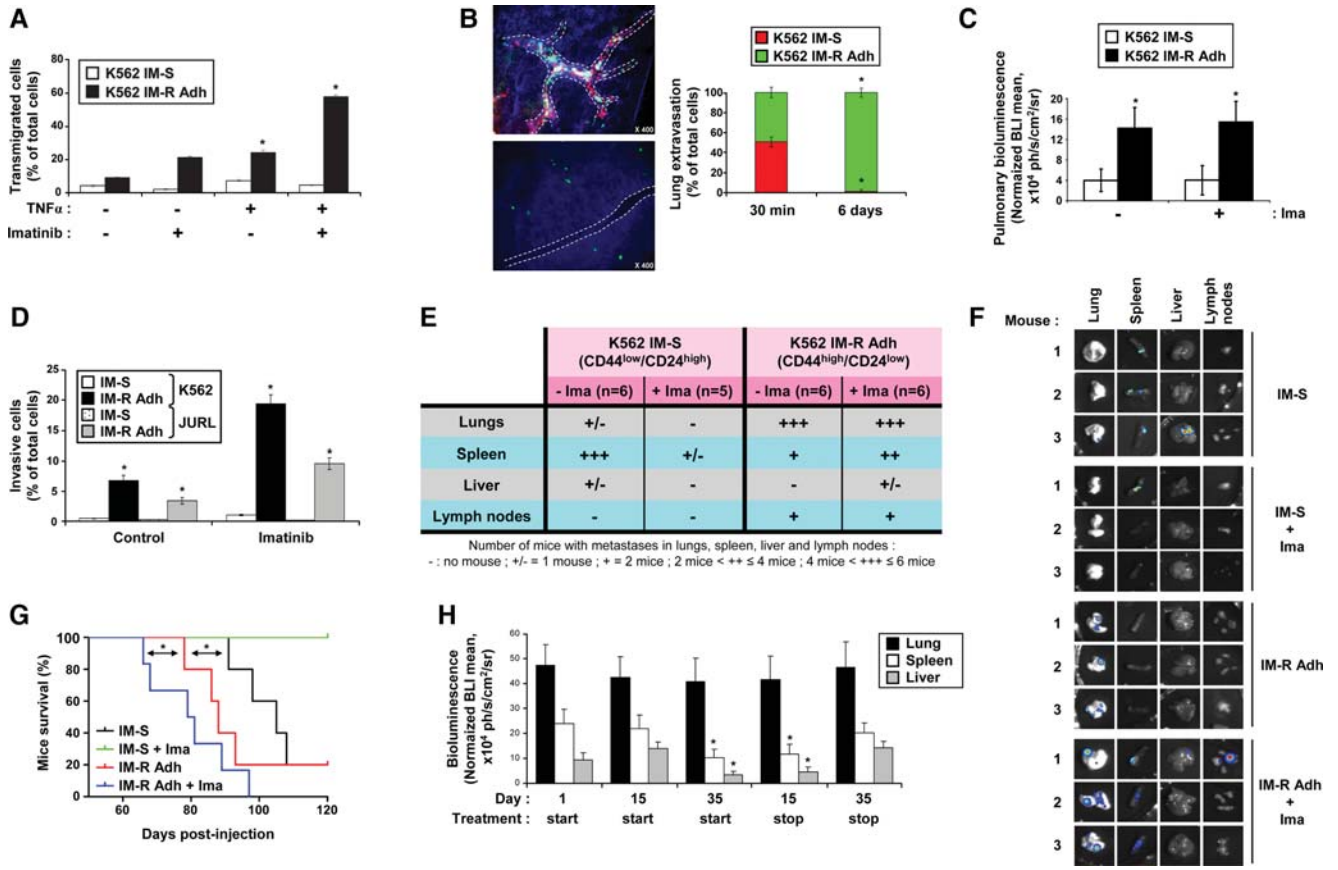

Figure 3 An EMT-initiating cell-like phenotype confers on IM-R Adh cells the ability to extravasate and invade in response to imatinib. (**A**) K562 IM-S and IM-R Adh cells were treated (or not) with imatinib (3 μM) and seeded onto a Boyden chamber coated with a primary endothelial (HUVEC) cell monolayer that has been pretreated (or not) with 10 ng/ml TNFα. After 24 h, the number of transmigrated cells was counted in the lower chamber by flow cytometry. The results are expressed as the percentage of migrated cells versus the total number of cells and represent the mean ± SD of four independent experiments performed in quadruplicate. (**B**) A total of 1.5×10^6 green IM-R Adh cells and red IM-S cells were injected via the tail vein of nude mice. At each indicated time point, blue dextran was administered before mice were sacrificed, and extravasated cells were counted using an inverted microscope. Two characteristic images are shown. The dotted white line indicates the blood vessels. (**C**) The pulmonary extravasation of K562 IM-S and IM-R Adh luciferase-positive cells was measured by bioluminescence imaging 4 days after tail vein injection. The nude mice in different cohorts ($n = 6$) were pretreated (or not) with imatinib (60 mg/kg). No significant differences were detected between the treated and untreated conditions. A significant difference of pulmonary extravasation potential was observed between IM-R Adh and IM-S cells. The results represent the mean pulmonary bioluminescence intensity ± SD. (**D**) K562 or JURL-MK1 IM-S and IM-R Adh counterparts were treated (or not) with imatinib (3 μM) and seeded onto a Matrigel-coated Boyden chamber for the invasion assay. After 24 h, the number of invading cells was determined in the lower chamber using flow cytometry. The results are expressed as the percentage of invasive cells versus the total number of cells and represent the mean ± SD of four independent experiments performed in quadruplicate. (**E** and **F**) After injection of 1×10^6 K562 IM-S and IM-R Adh cells into the tail vein, the nude mice were separated into four groups (as indicated in each column of the table) and treated (or not) with imatinib (60 mg/kg) for 70 days. The mice were sacrificed, and organs were harvested. The bioluminescence resulting from the presence of metastases was quantified with a Photon Imager. The metastatic tropism and invasiveness of IM-R Adh cells were compared with IM-S cells. The number of luciferase-positive mice for each organ is indicated in **E**. A characteristic image is shown for each organ in **F** (3 mice per group). (**G**) The Kaplan–Meier survival curves are shown for nude mice that received IM-S or IM-R Adh cells with or without imatinib treatment. (**H**) After tail-vein injection of IM-R Adh cells, the nude mice were treated with imatinib at day 15 or day 35 post-injection (start). Otherwise, treatment was dispensed at day 0 but stopped at day 15 or day 35 post-injection (stop). The positive-control mice were treated for 70 days. The results represent the mean bioluminescence intensity ± SD. For each panel of this figure, $*P < 0.05$ was considered significant.

proportion in the caudal vein of nude mice, and their ability to extravasate through the pulmonary parenchyma was evaluated (Figure 3B). We postulated that K562 IM-S cells would enter the venous system and migrate across the vascular endothelium in the lungs. As shown in Figure 3B, after 6 days, only the green IM-R Adh cells extravasated and represented almost 100% of the CML cells present in the lungs. These results were confirmed by using IM-S and IM-R Adh CML cells stably expressing luciferase. The mice were randomized into four groups ($n = 6$ per group) injected with IM-S or IM-R Adh cells and were then treated daily with an intraperitoneal injection of imatinib. Accordingly, 4 days after cell injection, bioluminescence was

detected in the lungs of all mice. Importantly, a 4-fold increase in bioluminescence intensity was observed in the lungs of mice injected with IM-R Adh cells, reflecting the increased capacity of these cells to extravasate *in vivo* (Figure 3C).

In addition, imatinib also increased the ability of JURL-MK1 and K562 IM-R Adh cells to invade a Matrigel barrier (Figure 3D). This increased invasive potential correlated with higher levels of MMP-2 and -9 expression, secretion and/or activation into the medium of IM-R Adh cells compared with IM-S cells (Supplementary Figure S5A and B). Finally, to evaluate *in vivo* the invasive behavior and metastatic tropism of IM-R Adh cells, we injected IM-S and IM-R Adh cells into mice via the tail vein and determined by bioluminescence imaging the preferential sites of metastases following long-term treatment with imatinib. Interestingly, K562 IM-S cells metastasized preferentially to the spleen, whereas, according to extravasation experiments, $CD44^{high}/CD24^{low}$ IM-R Adh cells displayed a pulmonary metastatic tropism. Finally, treatment of mice with imatinib inhibited tumor progression when using IM-S K562 cells (four out of five mice did not exhibit any bioluminescence-positive metastases) but exacerbated the aggressiveness of IM-R Adh cells that were capable of invading the spleen and lymph nodes in addition to the lungs (Figure 3E and F). This remarkable IM-R Adh cell aggressiveness is illustrated with Kaplan-Meier curves (Figure 3G) showing a significant decrease in mouse survival after IM-R Adh cell injection compared with IM-S cells. Imatinib treatment significantly enhanced IM-R Adh cell aggressiveness as observed by the short latency of CML disease. We also wished to determine whether this IM-R Adh cell population had a sustained aggressive potential following imatinib withdrawal. As depicted in Figure 3H, a late start (at day 35 post-injection) or an early stop (at day 15 post-injection) of imatinib therapy failed to block the tropism of IM-R Adh into the lungs but significantly diminished their invasion into the spleen and the liver. However, a late stop of imatinib treatment (at day 35 post-injection) did not impair their capacity to invade the spleen and liver. Consequently, imatinib appears to drive the initial tropism of IM-R Adh cells into the spleen and the liver but not into the lungs.

αVβ3 receptor is the primary mediator of the aggressive properties of $CD44^{high}/CD24^{low}$ CML Adh cells

Because IM-R Adh cells were tightly adhered to FN in the presence of imatinib, we screened by qPCR analysis the expression levels of a large panel of adhesion molecules in both parental K562 IM-S and IM-R Adh cells and validated their upregulated expression by flow cytometry and western blot analyses (Figure 4A and B). Increased expression levels of integrin (ITG)α2b, ITGβ3, ITGαV and PECAM1 were consistently detected in K562 IM-R Adh cells (Figure 4A and B), and overexpression of ITGβ3 was also confirmed in JURL-MK1 IM-R Adh cells (Figure 4C). Importantly, overexpression of ITGβ3 and PECAM1 but not ITGβ5 was detected in the PBMC of 10 CML patients in partial cytogenetic response after 1 year of imatinib therapy (Figure 4D and not shown), and the αVβ3 receptor is highly expressed on the surface of $CD34^{+}$ cells from imatinib-non-responder patients (Figure 4E). Given that some integrin clusters are up-regulated at the transcriptional level in IM-R Adh cells, we hypothesized that adhesive marker promoters were demethylated in this cell subpopulation. A screening by qPCR microplates of most adhesion molecules was performed on IM-S cells treated by 5-aza-2′-deoxycytidine (5Aza-dc, AZA), a DNA methylation inhibitor (Supplementary Figure S6). After 6 days of AZA-treatment, all integrin markers involved in IM-R Adh cells adhesion were increased in IM-S cells, suggesting that ITGβ3 and ITGαV promoters are demethylated in IM-R Adh cells.

Using loss-of-function approaches, we next investigated which of these adhesion-specialized proteins could be the primary mediator responsible for the adhesiveness and invasion functions related to the $CD44^{high}/CD24^{low}$ phenotype. The adhesive properties of K562 and JURL-MK1 IM-R Adh cells were impaired in the presence of an anti-β3, an anti-αV or an anti-αVβ3 receptor mAb, as were the adherence and invasiveness of these IM-R Adh cells treated with various concentrations of an RGD peptide (Figure 4F and G). In contrast, neither an anti-ITGβ1 mAb nor ITGβ5 knockdown abrogated IM-R Adh cell adhesion (Supplementary Figure S7A and B). Altogether, our findings highlight the crucial role of the αVβ3 receptor in promoting the adhesive and invasive phenotype of IM-R Adh CML cells in response to imatinib.

BCR-ABL phosphorylation was inhibited to the same extent by imatinib in IM-S and IM-R Adh cells, eliminating the possibility of a mutation in the kinase domain of BCR-ABL. However, sustained activation of ERK and an increased activation of FAK/Akt were detected in imatinib-stimulated IM-R Adh cells versus their IM-S counterparts (Figure 5A). In addition, we detected a clear colocalization of ITGβ3 and active FAK in the focal adhesion points of the spread K562 and JURL-MK1 IM-R Adh cells treated with imatinib (Figure 5B and Supplementary Figure S8), suggesting a specific role for the ITGβ3/FAK pathway following imatinib-induced spreading of IM-R Adh cells. As active FAK colocalized with ITGβ3 in focal adhesion points, we next investigated whether this kinase was involved in the adhesion of and invasion by IM-R Adh cells. The inhibition of FAK expression with two specific siRNAs (FAK1 and FAK2; Figure 5C) abrogated imatinib-mediated invasion by IM-R Adh cells (Figure 5D).

Given the known role of the ABL protein in modulating the F-actin cytoskeleton (Woodring et al., 2002), we hypothesized that ABL rather than BCR-ABL could be involved in promoting the effects of imatinib on IM-R Adh cell spreading and adhesion. To investigate this possibility, we first used two siRNAs directed against ABL (ABL1 and ABL2), which efficiently inhibit both BCR-ABL and ABL expression (Figure 5E). Joint silencing of BCR-ABL and ABL failed to affect the persistent activation of ERK and imatinib-induced FAK activation in IM-R Adh cells (Figure 5E), and both siRNAs increased the spreading, adhesive and invasive properties of these cells (Figure 5F and G). In contrast, increased adhesion of IM-R Adh cells was not observed when we used an shRNA that specifically abrogates BCR-ABL but not ABL expression (Figure 5H and I). Collectively, these data show that inhibition of ABL, but not BCR-ABL, is required to exacerbate the adhesive properties of $CD44^{high}/CD24^{low}$ IM-R Adh cells.

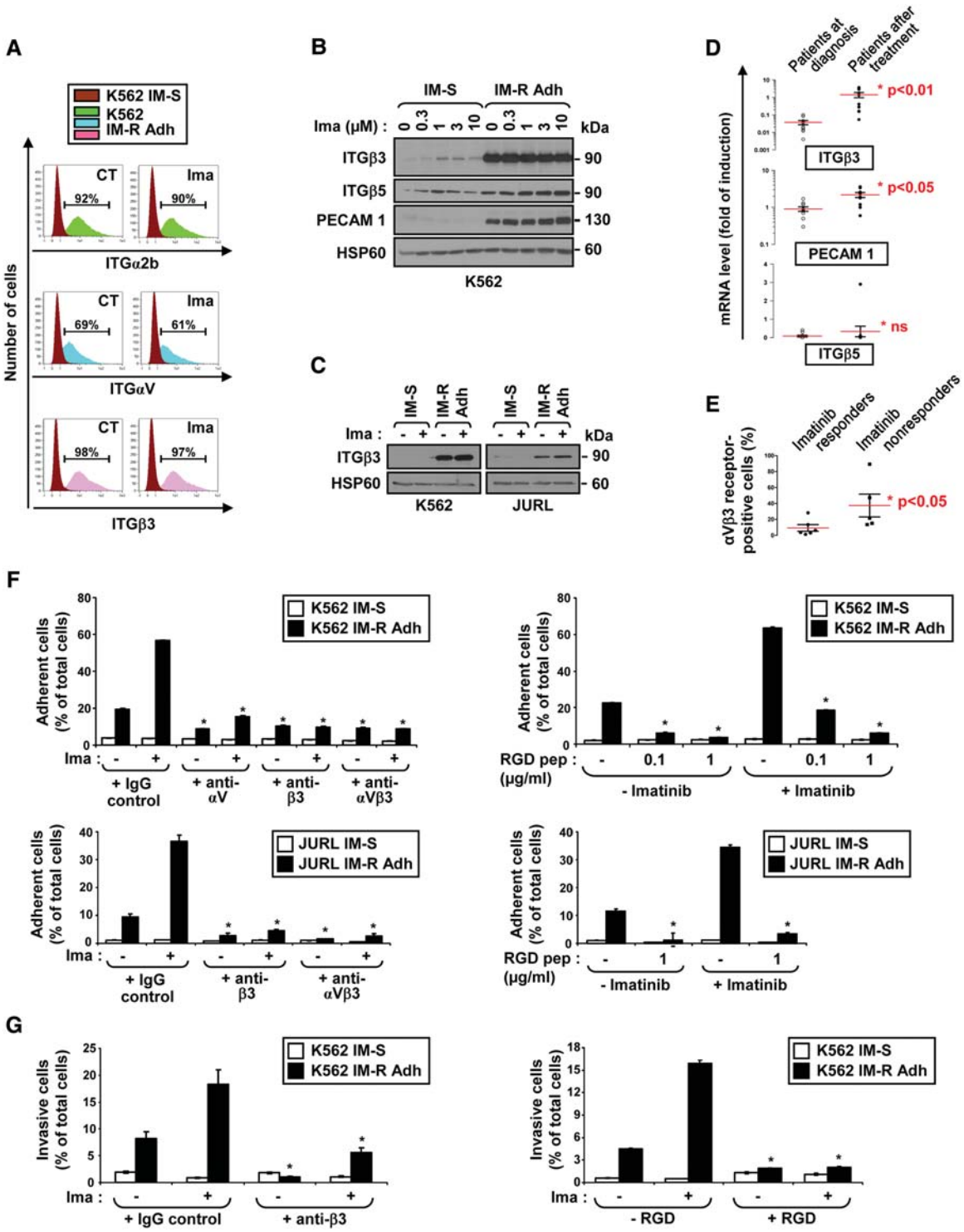

Figure 4 Overexpression of αVβ3 is sufficient to mediate the adhesion of and invasion by IM-R Adh cells. (**A**–**C**) The protein expression levels of integrins were analyzed by flow cytometry (**A**) and immunoblotting (**B** and **C**) using specific antibodies. (**D**) Q-PCR analysis of various adhesion markers was performed on CML cells from 10 patients at diagnosis or in partial cytogenetic response after one year of therapy with imatinib. (**E**) The expression levels of the αVβ3 receptor at the membrane of $CD34^+$ CML cells from imatinib-responder ($n = 5$) and non-responder patients ($n = 5$) were quantified by flow cytometry. (**F** and **G**) IM-S and IM-R Adh K562 and JURL-MK1 cells were preincubated for 15 min in the presence or the absence of either IgG isotype control, anti-ITGαV, anti-ITGβ3 or anti-αVβ3 receptor mAb neutralizing antibodies (1 μg/ml) (**F**, left panel) or with indicated concentrations of an RGD peptide (**F**, right panel) and then incubated with imatinib (3 μM) for 16 h. (**G**) The number of invasive cells was assessed as described in Materials and methods. The results in **F** and **G** are expressed as the percentage of adherent or invasive cells versus the total number of cells and represent the mean ± SD of four independent experiments performed in quadruplicate. For each panel of this figure, *$P < 0.05$ was considered significant. * ns was considered as non-significant.

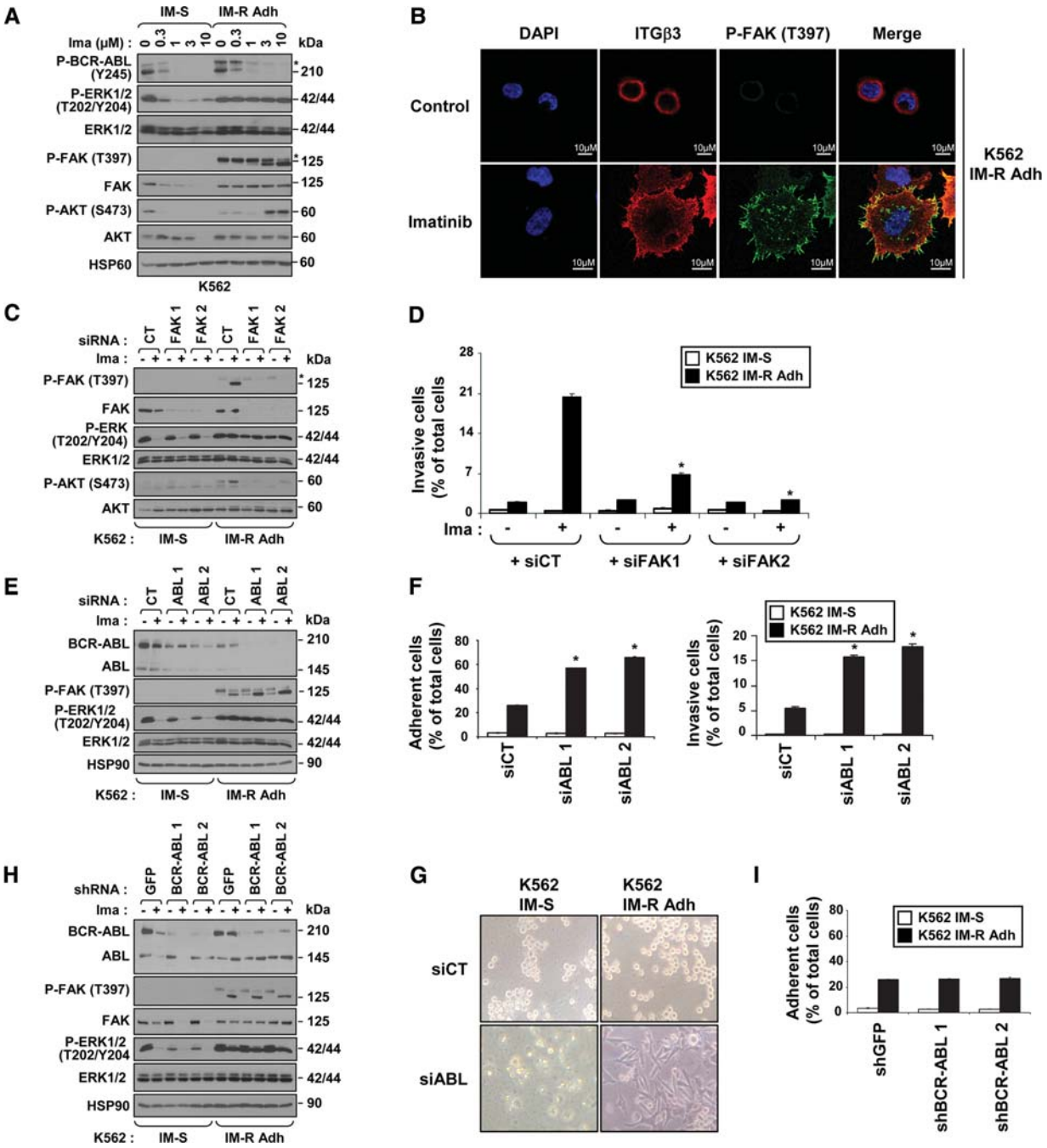

Figure 5 Imatinib-induced spreading of IM-R Adh cells is dependent on ABL but not BCR-ABL and mediates FAK/Akt pathway activation. (**A**) IM-S and IM-R Adh K562 cells were stimulated with increasing concentrations of imatinib for 24 h. BCR-ABL, ERK1/2, Akt, FAK and HSP60 (loading control) protein levels were visualized by immunoblotting. An asterisk indicates a non-specific band associated with the anti-FAK mAb. (**B**) K562 IM-R Adh cells were treated with 3 μM imatinib for 30 min. Then, glass coverslips were fixed and stained with an anti-ITGβ3 antibody (red), an anti-phospho-FAK antibody (green) and 1 mg/ml DAPI (blue). The immunostained cells were analyzed by confocal microscopy. (**C** and **D**) IM-S and IM-R Adh K562 cells were transfected for 3 days with a control siRNA or two siRNAs directed against FAK and treated with imatinib (3 μM). After 24 h, FAK, AKT and ERK1/2 levels and phosphorylation levels were visualized by immunoblotting (**C**) and the number of invasive cells was assessed (**D**). (**E**–**G**) IM-S and IM-R Adh K562 cells were transfected for 3 days with a control siRNA (siCT) or two siRNAs directed against ABL (siABL 1 and 2). Imatinib was added for the last 16 h. (**E**) BCR-ABL, ABL, FAK, and ERK1/2 levels and phosphorylation levels were visualized by immunoblotting using specific antibodies. HSP90 was used as a loading control. (**F**) The number of adhesive, migrating and invasive cells was assessed as described in Figure 1. (**G**) The images of representative plates are shown. (**H** and **I**) IM-S and IM-R Adh K562 cells were transfected for 3 days with a control shRNA (GFP) or two shRNAs specifically directed against BCR-ABL (shBCR-ABL 1 and 2). Imatinib was added for the last 16 h. (**H**) BCR-ABL, ABL, FAK, and ERK1/2 levels and phosphorylation levels were visualized as described in **E**. (**I**) The number of adhesive cells was evaluated. The results in **D**, **F**, and **I** are expressed as the percentage of adherent cells versus total number of cells and represent the mean ± SD of four independent experiments performed in quadruplicate. For each panel of this figure, $*P < 0.05$ was considered significant.

αVβ3-mediated adhesion of CD44^{high}/CD24^{low} IM-R Adh cells is also involved in resistance to imatinib through the induction of a CAM-DR process

CAM-DR is a multidrug-resistant phenotype associated with cell–cell or cell–matrix interactions (Damiano, 2002). To investigate whether overexpression of αVβ3 was responsible for the protection of IM-R Adh cells from imatinib-mediated apoptosis, a hallmark of CAM-DR, we used either low-adhesive uncoated plates or an anti-β3 blocking mAb. As expected, FAK was not activated in K562 IM-S cells compared with K562 IM-R Adh cells treated with imatinib (Figure 6A). Failure of ITGβ3 engagement, by seeding cells on uncoated plates or by using a blocking antibody, impaired imatinib-induced FAK/Akt phosphorylation and constitutive ERK1/2 activation and resensitized IM-R Adh cells to imatinib-induced caspase 3 activation (Figure 6B). These results were confirmed using a RGD peptide that was shown to block imatinib-induced FAK phosphorylation and persistent ERK activation and trigger caspase 3 activation (Figure 6C) and PARP cleavage (Figure 6D) in imatinib-treated K562 IM-R Adh cells.

Finally, it was important to investigate whether overexpression of ITGαV, ITGβ3 or the combination of ITGαV and ITGβ3 was sufficient to confer enhanced adhesive properties to IM-S cells and

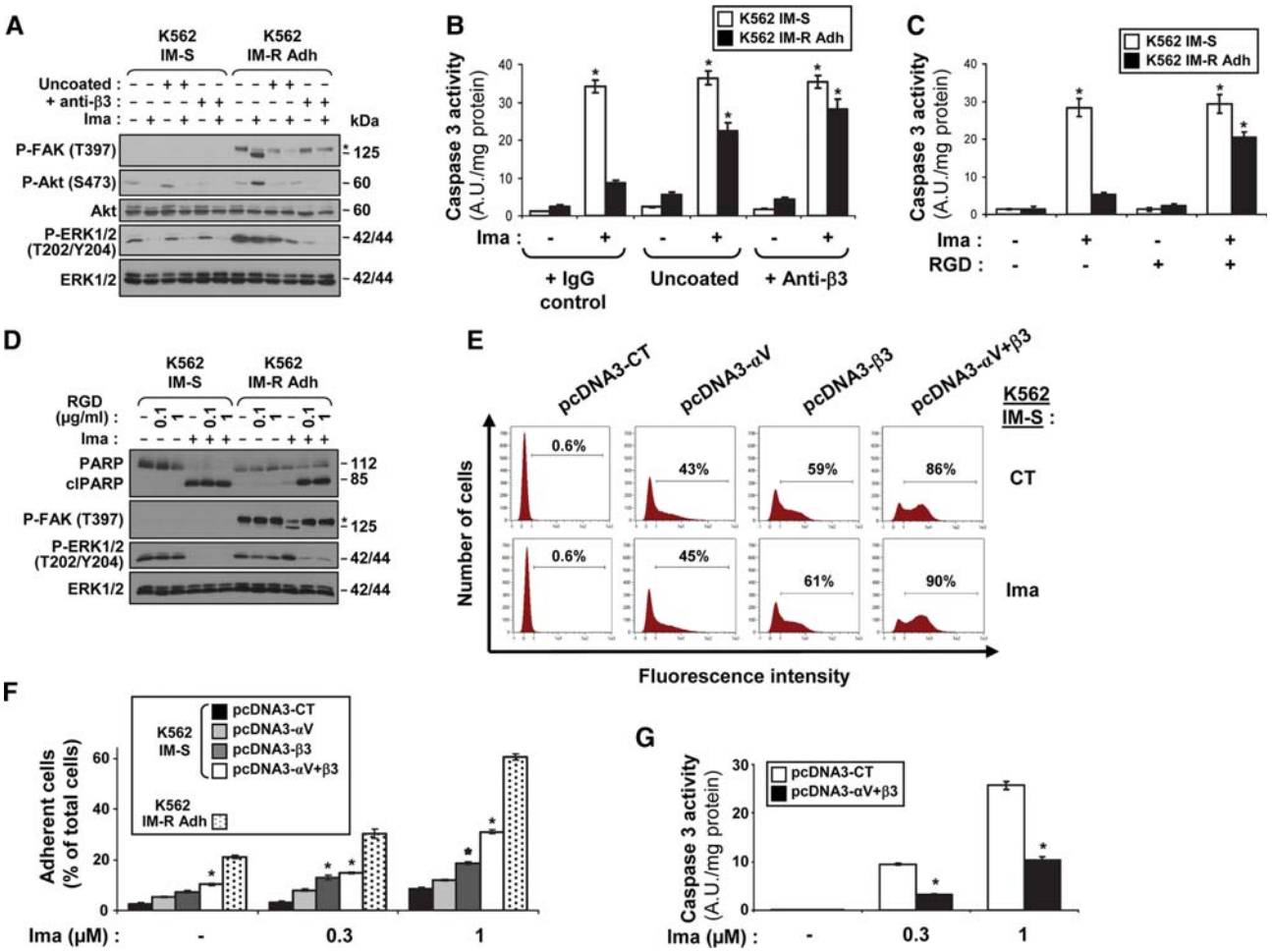

Figure 6 Inhibition of αVβ3 receptor engagement resensitizes IM-R Adh cells to imatinib-induced apoptosis. (**A**–**D**) IM-S and IM-R Adh K562 cells were plated on coated or uncoated wells or treated with either 1 μg/ml IgG isotype control, an anti-ITGβ3 mAb neutralizing antibody (**A**) or the indicated concentrations of an RGD peptide (**C**). The cells were further exposed to 3 μM imatinib for the next 48 h. (**A** and **D**) FAK, Akt and ERK1/2 levels and phosphorylation status were visualized with immunoblotting using specific antibodies. (**B** and **C**) Caspase 3 activity was assessed using z-DEVD-AMC as substrate. The results are expressed as arbitrary units (A.U.) per mg of protein and represent the mean ± SD of four independent experiments performed in quadruplicate. (**E**–**G**) IM-S K562 cells (1×10^5/ml) were transfected with a pcDNA3-Control (pcDNA3-CT), a pcDNA3-ITGαV (pcDNA3-αV), a pcDNA3-ITGβ3 (pcDNA3-β3) or with both ITGαV and ITGβ3 vectors (pcDNA3-αV+β3) for 3 days. The cells were then treated with two concentrations of imatinib for the last 16 h before visualization of integrin receptor overexpression by FACS (**E**) or determination of adhesion as described above (**F**). IM-R Adh cells were used as a positive control for adhesion. The results are expressed as the percentage of adherent cells of the total number of cells and represent the mean ± SD of four independent experiments performed in quadruplicate. (**G**) At 36 h after transfection, the indicated concentrations of imatinib were added for the next 36 h. Caspase 3 activity was assessed using z-DEVD-AMC as a substrate. The results are expressed as arbitrary units per mg of protein and represent the mean ± SD of four independent experiments performed in quadruplicate. For each panel of this figure, *$P < 0.05$ was considered significant.

resistance to imatinib-induced apoptosis. The co-expression of ITGαV and β3 allowed most cells to express high levels of integrin at the membrane (Figure 6E) and induced maximal adhesion (60%, which is similar to the level reached in K562 IM-R Adh cells) in the presence of imatinib (Figure 6F). Importantly, co-expression of αVβ3 integrin at the cell surface was sufficient to inhibit imatinib-mediated apoptosis (Figure 6G). Collectively, our findings show that IM-R Adh cells are resistant to imatinib through ITGβ3-mediated CAM-DR.

Discussion

Recent studies have highlighted the existence within tumors, of a small subpopulation of cancer stem/initiating cells (CSCs) that are thought to be the driving force involved in carcinogenesis, local invasion and the metastatic process (Glinsky, 2005; Spillane and Henderson, 2007). Moreover, accumulating data support the idea that these cells could play an important role in chemoresistance (Dean et al., 2005). Therefore, these highly chemoresistant cells are likely to be the main cause of relapse after an initial favorable response to a chemotherapeutic treatment. To mimic *in vitro* the emergence of such a cell subpopulation in response to TKIs, we first generated imatinib-resistant cells by iteratively exposing cells to low doses of imatinib. When maintained in the continuous presence of high concentrations of imatinib, we observed that a small spread population of IM-R CML cells strongly adhered to the culture dishes and continued to proliferate as attached cells. After several cycles of gentle detachment and replating, homogeneous populations of K562 and JURL-MK1 IM-R adherent cells were obtained. Upon withdrawal of imatinib, IM-R Adh cells quickly stopped spreading and became round with a very slight adhesion phenotype, demonstrating that the enhanced adhesion of IM-R Adh CML cells is strictly dependent on the presence of imatinib in the culture medium.

An interesting feature of the IM-R Adh CML cells described here is that they exhibited an increased potential for migration and invasion. In the presence of imatinib, they displayed the same spread morphology, high migratory and invasive behavior and expressed the same set of mesenchymal markers (SNAIL, osteonectin, TBX3, FN and β-catenin) that cells undergoing the EMT express to migrate from one tissue to another (Thiery et al., 2009). Assuming that, owing to their non-epithelial origin, IM-R Adh CML cells have not undergone a true EMT process, we postulated that they exhibited a behavior similar to that of EMT cells and can therefore be considered as displaying an EMT-like phenotype.

In solid cancers (more particularly in breast tumors), CSCs are defined as $CD44^{high}/CD24^{low}$ cells that have acquired an increased invasive capacity owing to their ability to undergo EMT (Al-Hajj et al., 2003). Interestingly, we found that the IM-R Adh population was 11-fold enriched with LIC compared with IM-S cells and had upregulated CD44 mRNA and downregulated CD24 mRNA, a property shared by breast cancer-initiating/stem cells. Accordingly, this $CD44^{high}/CD24^{low}$ subpopulation is also present among CML primary cells from imatinib-non-responder patients. More importantly, when injected *in vivo* into nude mice, $CD44^{high}/CD24^{low}$ IM-R Adh CML cells extravasated four times higher to the lung than their $CD44^{low}/CD24^{high}$ IM-S counterparts. In addition, dissemination of $CD44^{high}/CD24^{low}$ CML cells in lymphoid organs, such as the spleen or lymph nodes, was increased in cells treated with imatinib, a situation that reflects the one observed *in vitro*. This imatinib-induced invasiveness of IM-R Adh cells results in a drastic reduction in mouse survival compared with the survival observed after IM-S cell injection. Collectively, these results show that long-term exposure to imatinib promotes a small population of leukemic cells that exhibit a stemness EMT-like phenotype compatible with a transdifferentiation process. In addition, this observation also suggests that it could be beneficial for patients to avoid long-term treatment with BCR-ABL-only TKI therapies such as imatinib or nilotinib in favor of a broader therapy. However, our results also suggest that halting imatinib therapy after a long period of time is not sufficient to prevent the emergence of this $CD44^{high}/CD24^{low}$ CML cell population, as the tropism of these cells for their target organs is driven at the beginning of TKI-treatment.

To further characterize this EMT-like phenotype and to determine the molecular players responsible for the exacerbated adhesive and invasive properties associated with this cell phenotype, we compared the integrin signature of K562 and JURLMK-1 IM-R Adh cells with that of parental CML cells. IM-R Adh cells showed a drastic increase in the expression of several adhesion molecules such as TSP1, TSP1-R, ITGα2B, ITGα5, ITGαV, ITGβ1, ITGβ3, ITGβ5, MCAM, and PECAM1. Interestingly, overexpression of some of these molecules such as ITGβ3 was also observed in the PBMC cells from CML patients treated after 1 year of imatinib therapy. Our data suggest that high expression of this set of integrins in the IM-R Adh cell population results from promoter demethylation.

Whereas ITGβ1 allows for interactions between normal $CD34^{+}$ progenitors and the medullar stroma to control proliferation and limit migration, it has previously been reported that α4β1 (VLA-4) and α5β1 (VLA-5)-mediated adhesion of $CD34^{+}$ cells is perturbed during CML-associated transformation (Verfaillie et al., 1992). This alteration of adhesive properties of CML progenitors is mediated by BCR-ABL, which blocks both the engagement of VLA-4 and VLA-5 and signaling via these receptors (Bhatia and Verfaillie, 1998). Interestingly, in this context, AG957, the first TKI shown to be effective on BCR-ABL, allowed restoration of CML cell adhesion to FN (Bhatia et al., 1998). However, whereas ITGα5 and ITGβ1 are overexpressed in IM-R Adh cells, they are definitely not involved in the imatinib-mediated spreading of these cells. Rather, adhesion of IM-R Adh cells was found to be dependent on a functional αVβ3 integrin receptor (CD51/CD61) as it was impaired in the presence of an RGD peptide, anti-β3, anti-αV, or anti-αVβ3 mAbs. Thus, IM-R Adh cells exhibit an EMT-like phenotype favoring the expression of a new panel of integrins (particularly αVβ3) and molecules involved in intercellular adhesion. It may appear paradoxical that increased adhesion is associated with a highly migratory and invasive phenotype. However, it is now understood that adhesion serves as a molecular clutch to promote cell migration (Huttenlocher and Horwitz, 2011). First, integrin-induced traction forces orchestrate cell movement by linking the extracellular substratum (i.e. fibronectin) to the actin cytoskeleton, which we observed (with

phalloidin staining) to be completely reorganized. Second, ligand binding induces integrin clustering that forms the multiprotein complex necessary to activate the multiple signaling pathways (i.e. FAK and ILK pathways) involved in cell migration. Finally, it has been reported that the integrin repertoire expressed by cells strongly correlates with migratory behavior; for example, expression of αVβ3 integrin on melanomas correlates with tumor invasion (Seftor et al., 1992).

Acquisition of this new set of integrins confers on IM-R Adh cells the ability to overcome ITGβ1-mediated alteration of adhesive properties and drives a high invasive potential in response to imatinib. Consistent with this ITGβ1-independent mode of adhesion and invasion, we show that inhibition of BCR-ABL, described as the main factor blocking ITGβ1-mediated adhesion in CML (Bhatia et al., 1998), failed to increase adhesion of IM-R Adh. In contrast, inactivation of ABL function with imatinib or specific siRNAs strongly enhanced adhesion and invasion following cellular spreading. Recent studies have reported that inhibition of ABL in NIH3T3 cells triggered cellular spreading following activation of two key substrates, CrkII and Nck, that control reorganization of the actin cytoskeleton (Antoku et al., 2008). Whether this is also the case in our cellular model requires further investigation. Nevertheless, imatinib-mediated spreading is associated with cytoskeleton reorganization, which controls the clustering of αVβ3 and the formation of focal adhesion points responsible for the activation of the FAK/Akt pathway necessary for transendothelial migration and invasion.

An EMT-like phenotype of IM-R Adh cells does not explain why imatinib failed to kill them. It has been demonstrated that tumor cell interactions with FN or more generally with other ECM molecules, considerably affect drug response and are critical for the establishment of drug-resistant cell populations in leukemia (Damiano et al., 1999; Damiano and Dalton, 2000). Therefore, forced adhesion of the K562 CML cell line to FN via α5β1 integrin engagement was reported to significantly impair imatinib-induced apoptosis (Lundell et al., 1996). This process, referred to as CAM-DR, was initially reported in multiple myeloma cells by Damiano et al. (1999).

In the present study, using loss-of-function approaches with neutralizing antibodies or an RGD peptide, we determined that the EMT-like phenotype acquired by IM-R Adh cells confers an αVβ3-dependent invasive potential and cell adhesion-mediated imatinib resistance (CAM-IR). In Damiano's work, the authors report CAM-DR as a process resulting from chemotherapy-induced overexpression of integrin subunits that mediate chemoresistance via cellular adhesion. In addition, imatinib directly or indirectly increases expression of adhesive molecules that by themselves promote enhanced adhesion and subsequently drug resistance. Therefore, the CAM-DR process can be defined as the sum of a drug-induced cellular switch and resistance to this drug. The cellular switch process cannot be dissociated from the resistance mechanism.

We next investigated the signaling pathways activated downstream of the αVβ3 receptor responsible for CAM-IR. While imatinib-mediated cellular spreading triggered the FAK/Akt pathway involved in the migration of and invasion by IM-R Adh cells, we also observed a constitutive activation of the ERK pathway independent of imatinib. Importantly, despite BCR-ABL inhibition by imatinib, the ERK pathway was activated by αVβ3 receptor engagement in IM-R Adh cells. Accordingly, a blockade of αVβ3 or inhibition of the ERK pathway by U0126 (not shown) resensitized IM-R Adh cells to imatinib-mediated cell death. This observation is in good agreement with recent data in the literature that involved several cell adhesion-mediated survival pathways including VLA-4/MEK in CAM-DR (Chatterjee et al., 2004).

In conclusion, Supplementary Figure S9 summarizes the mechanism of action of imatinib on the small subpopulation of $CD44^{high}/CD24^{low}$ CML cells. In $CD34^{+}$ CML cells, BCR-ABL triggers the inhibition of ITGB1 clustering and signaling to promote de-adhesion from BM stromal cells and the systemic circulation of CML cells (Verfaillie et al., 1997). A rare $CD44^{high}/CD24^{low}$ subpopulation selected by continuous imatinib exposure displaying an EMT stem cell-like phenotype and expressing a new set of adhesion markers and, more particularly, αVβ3 receptor spreads and invades in response to TKI treatment. Interestingly, imatinib-induced ABL inhibition promotes the clustering of αVβ3 and formation of focal adhesion points responsible for the activation of the FAK/Akt pathway favoring invasion and extravasation. Despite imatinib-mediated BCR-ABL inhibition, αVβ3 receptor signaling also maintains the constitutive activation of ERK1/2 that is involved in CAM-IR.

Because CAM-DR has been recognized as an important mechanism of resistance to chemotherapy in hematopoietic malignancies and solid cancers, anti-adhesion strategies aimed at circumventing such resistances have received increasing attention. These anti-adhesion strategies include the targeting of surface antigens, the inhibition of cell adhesion-associated pathways, the inhibition of CAM-DR and targeted drug delivery. The demonstration of the existence of a rare EMT-like subpopulation of CML cells that overexpresses the αVβ3 receptor to resist TKI treatment may represent the starting point for the use of anti-adhesion therapies in hematopoietic malignancies where CAM-DR is activated. In this respect, treating patients with a combination of TKI-inhibitors and anti-adhesion molecules (i.e. humanized anti-ITGβ3 antibodies) or FAK inhibitors to prevent the occurrence of rare cell populations with high invasive potential could represent an original therapeutic strategy.

Materials and methods

Reagents and antibodies

The list of antibodies and reagents used in this manuscript is provided in Supplementary Materials and methods.

Cell lines

The human CML cell lines K562 (ATCC) and JURL-MK1 (DSMZ) were grown at 37°C under 5% CO_2 in RPMI 1640 medium (Gibco BRL) supplemented with 5% and 10% fetal calf serum (Gibco), respectively. The procedure to isolate IM-R Adh cell population is described in Supplementary Materials and methods.

Primary cell isolation and real-time qPCR analysis

Blood samples were collected from 10 patients newly diagnosed with CML or in partial cytogenetic response after one year of imatinib therapy as part of an institutionally approved

cellular sample collection protocol. Informed consent was obtained according to institutional guidelines. The sorted $CD34^+$ primary cells from imatinib-responder or non-responder patients were used for quantitative PCR analysis and flow cytometry and adhesion assays. The patients with a complete cytogenetic response within 1 year were defined as responders, and the patients lacking a major cytogenetic response (>35% Philadelphia-positive metaphases) after 1 year were defined as non-responders. The detailed protocol for treatment of primary cells is described in Supplementary Materials and methods.

Western blotting

Western blot analyses have been described previously (Puissant et al., 2010a, b).

Measurement of caspase 3 activity

Caspase assays have previously been described in detail (Puissant et al., 2008; Fenouille et al., 2010).

3D spheroid formation

10×10^4 K562 cells/ml were centrifuged at 400 *g* for 10 min. The pellet was gently detached in a medium supplemented with 1 mM $MnCl_2$ and 2 mM $MgCl_2$ and added to a 24-well plate coated with 1.5% agar (Difco; Sparks). The plates were then left to incubate for 48 h, by which time cells had organized into three-dimensional spheroids.

Confocal microscopy

The microscopy experiments procedure is detailed in Supplementary Materials and methods.

Knockdown by siRNA

Stealth® small interfering RNAs (siRNA) targeting FAK and Abl were purchased from Invitrogen. The plasmid controls pcDNA3-CT, pcDNA3-ITGαV (a generous gift from Dr Jean-Luc Coll, INSERM U823, Grenoble, France), and pcDNA3-ITGβ3 (a kind gift from Dr Ernst Lengyel, University of Chicago Medical Center, Chicago, IL, USA) were transfected using the Nucleofector® Amaxa (protocol T16 and Kit V; Lonza AG) (Puissant et al., 2010a, b).

Flow cytometry analysis

The cells were washed with ice-cold PBS, incubated for 30 min with the indicated anti-ITG antibodies diluted in PBS, 0.5% BSA, and 2 mM EDTA and analyzed using a MACSQuant.

Co-culture experiments

HUVEC primary endothelial cells were grown in EGM®-2 and were cultured on the upper membrane surface of a Boyden chamber overnight to generate a confluent monolayer. IM-S and IM-R Adh K562 cells were seeded into the HUVEC-coated Boyden chamber membrane pretreated (or not pretreated) with 10 ng/ml TNFα (Peprotech).

In vivo studies

Luciferase-positive leukemic cells were generated as described in Supplementary Materials and methods and visualized in the animal after intraperitoneal injection of 50 mg/kg luciferin (Caliper Life Sciences) by bioluminescence imaging using a Photon Imager (Biospace Lab). To perform pulmonary extravasation analysis, 1.5×10^6 IM-S and IM-R Adh cells were labeled with CellTracker™ Red and Green, respectively, and lungs analyzed as described in Supplementary Materials and methods.

Statistical analyses

The results are expressed as the mean ± SD. Statistical analyses for *in vitro* and *in vivo* experiments were performed as described in Supplementary Materials and methods.

Supplementary material

Supplementary material is available at *Journal of Molecular Cell Biology* online.

Acknowledgements

We acknowledge the C3M imaging Core Facility (MICA) and animal facility.

Funding

This work was supported by INSERM, INCA (Grant PL2006-126), and the Fondation de France (FDF). P.A. is the recipient of a Contrat Hospitalier de Recherche Translationnel (CHRT 2010–2013) with the CHU of Nice, France. A.P. is the recipient of a fellowship from the Association pour la Recherche sur le Cancer (ARC). A.J. is the recipient of a fellowship from the LNCC. G.R. has a fellowship from the Fondation de France (FDF).

Conflict of interest: none declared.

References

Ahmed, N., Abubaker, K., Findlay, J., et al. (2010). Epithelial mesenchymal transition and cancer stem cell-like phenotypes facilitate chemoresistance in recurrent ovarian cancer. Curr. Cancer Drug Targets *10*, 268–278.

Al-Hajj, M., Wicha, M.S., Benito-Hernandez, A., et al. (2003). Prospective identification of tumorigenic breast cancer cells. Proc. Natl Acad. Sci. USA *100*, 3983–3988.

Antoku, S., Saksela, K., Rivera, G.M., et al. (2008). A crucial role in cell spreading for the interaction of Abl PxxP motifs with Crk and Nck adaptors. J. Cell Sci. *121*, 3071–3082.

Bhatia, R., and Verfaillie, C.M. (1998). Inhibition of BCR-ABL expression with antisense oligodeoxynucleotides restores beta1 integrin-mediated adhesion and proliferation inhibition in chronic myelogenous leukemia hematopoietic progenitors. Blood *91*, 3414–3422.

Bhatia, R., Munthe, H.A., and Verfaillie, C.M. (1998). Tyrphostin AG957, a tyrosine kinase inhibitor with anti-BCR/ABL tyrosine kinase activity restores beta1 integrin-mediated adhesion and inhibitory signaling in chronic myelogenous leukemia hematopoietic progenitors. Leukemia *12*, 1708–1717.

Chatterjee, M., Stuhmer, T., Herrmann, P., et al. (2004). Combined disruption of both the MEK/ERK and the IL-6R/STAT3 pathways is required to induce apoptosis of multiple myeloma cells in the presence of bone marrow stromal cells. Blood *104*, 3712–3721.

Damiano, J.S. (2002). Integrins as novel drug targets for overcoming innate drug resistance. Curr. Cancer Drug Targets *2*, 37–43.

Damiano, J.S., and Dalton, W.S. (2000). Integrin-mediated drug resistance in multiple myeloma. Leuk. Lymphoma *38*, 71–81.

Damiano, J.S., Cress, A.E., Hazlehurst, L.A., et al. (1999). Cell adhesion mediated drug resistance (CAM-DR): role of integrins and resistance to apoptosis in human myeloma cell lines. Blood *93*, 1658–1667.

Damiano, J.S., Hazlehurst, L.A., and Dalton, W.S. (2001). Cell adhesion-mediated drug resistance (CAM-DR) protects the K562 chronic myelogenous leukemia cell line from apoptosis induced by BCR/ABL inhibition, cytotoxic drugs, and gamma-irradiation. Leukemia *15*, 1232–1239.

Dean, M., Fojo, T., and Bates, S. (2005). Tumour stem cells and drug resistance. Nat. Rev. Cancer *5*, 275–284.

Deininger, M.W., Goldman, J.M., and Melo, J.V. (2000). The molecular biology of chronic myeloid leukemia. Blood *96*, 3343–3356.

Druker, B.J., Talpaz, M., Resta, D.J., et al. (2001). Efficacy and safety of a specific inhibitor of the BCR-ABL tyrosine kinase in chronic myeloid leukemia. N. Engl. J. Med. *344*, 1031–1037.

Fenouille, N., Puissant, A., Dufies, M., et al. (2010). Persistent activation of the Fyn/ERK kinase signaling axis mediates imatinib resistance in chronic myelogenous leukemia cells through upregulation of intracellular SPARC. Cancer Res. *70*, 9659–9670.

Gires, O. (2011). Lessons from common markers of tumor-initiating cells in solid cancers. Cell Mol. Life Sci. *68*, 4009–4022.

Glinsky, G.V. (2005). Death-from-cancer signatures and stem cell contribution to metastatic cancer. Cell Cycle *4*, 1171–1175.

Groffen, J., Stephenson, J.R., Heisterkamp, N., et al. (1984). Philadelphia chromosomal breakpoints are clustered within a limited region, bcr, on chromosome 22. Cell *36*, 93–99.

Hope, K., and Bhatia, M. (2011). Clonal interrogation of stem cells. Nat. Methods *8*, S36–S40.

Hu, Y., and Smyth, G.K. (2009). ELDA: extreme limiting dilution analysis for comparing depleted and enriched populations in stem cell and other assays. J. Immunol. Methods *347*, 70–78.

Hurley, R.W., McCarthy, J.B., and Verfaillie, C.M. (1995). Direct adhesion to bone marrow stroma via fibronectin receptors inhibits hematopoietic progenitor proliferation. J. Clin. Invest. *96*, 511–519.

Huttenlocher, A., and Horwitz, A.R. (2011). Integrins in cell migration. Cold Spring Harb. Perspect. Biol. *3*, a005074.

Kai, K., Arima, Y., Kamiya, T., et al. (2010). Breast cancer stem cells. Breast Cancer *17*, 80–85.

Li, Z.W., and Dalton, W.S. (2006). Tumor microenvironment and drug resistance in hematologic malignancies. Blood Rev. *20*, 333–342.

Lundell, B.I., McCarthy, J.B., Kovach, N.L., et al. (1996). Activation-dependent alpha5beta1 integrin-mediated adhesion to fibronectin decreases proliferation of chronic myelogenous leukemia progenitors and K562 cells. Blood *87*, 2450–2458.

Mani, S.A., Guo, W., Liao, M.J., et al. (2008). The epithelial-mesenchymal transition generates cells with properties of stem cells. Cell *133*, 704–715.

Mego, M., Mani, S.A., and Cristofanilli, M. (2010). Molecular mechanisms of metastasis in breast cancer–clinical applications. Nat. Rev. Clin. Oncol. *7*, 693–701.

O'Brien, S.G., Guilhot, F., Larson, R.A., et al. (2003). Imatinib compared with interferon and low-dose cytarabine for newly diagnosed chronic-phase chronic myeloid leukemia. N. Engl. J. Med. *348*, 994–1004.

Puissant, A., Grosso, S., Jacquel, A., et al. (2008). Imatinib mesylate-resistant human chronic myelogenous leukemia cell lines exhibit high sensitivity to the phytoalexin resveratrol. FASEB J. *22*, 1894–1904.

Puissant, A., Colosetti, P., Robert, G., et al. (2010a). Cathepsin B release after imatinib-mediated lysosomal membrane permeabilization triggers BCR-ABL cleavage and elimination of chronic myelogenous leukemia cells. Leukemia *24*, 115–124.

Puissant, A., Robert, G., Fenouille, N., et al. (2010b). Resveratrol promotes autophagic cell death in chronic myelogenous leukemia cells via JNK-mediated p62/SQSTM1 expression and AMPK activation. Cancer Res. *70*, 1042–1052.

Salesse, S., and Verfaillie, C.M. (2002). Mechanisms underlying abnormal trafficking and expansion of malignant progenitors in CML: BCR/ABL-induced defects in integrin function in CML. Oncogene *21*, 8605–8611.

Seftor, R.E., Seftor, E.A., Gehlsen, K.R., et al. (1992). Role of the alpha v beta 3 integrin in human melanoma cell invasion. Proc. Natl Acad. Sci. USA *89*, 1557–1561.

Sheridan, C., Kishimoto, H., Fuchs, R.K., et al. (2006). $CD44^{+}/CD24^{-}$ breast cancer cells exhibit enhanced invasive properties: an early step necessary for metastasis. Breast Cancer Res. *8*, R59.

Shet, A.S., Jahagirdar, B.N., and Verfaillie, C.M. (2002). Chronic myelogenous leukemia: mechanisms underlying disease progression. Leukemia *16*, 1402–1411.

Spillane, J.B., and Henderson, M.A. (2007). Cancer stem cells: a review. ANZ J. Surg. *77*, 464–468.

Steelman, L.S., Pohnert, S.C., Shelton, J.G., et al. (2004). JAK/STAT, Raf/MEK/ERK, PI3K/Akt and BCR-ABL in cell cycle progression and leukemogenesis. Leukemia *18*, 189–218.

Thiery, J.P. (2002). Epithelial-mesenchymal transitions in tumour progression. Nat. Rev. Cancer *2*, 442–454.

Thiery, J.P., Acloque, H., Huang, R.Y., et al. (2009). Epithelial-mesenchymal transitions in development and disease. Cell *139*, 871–890.

Verfaillie, C.M., McCarthy, J.B., and McGlave, P.B. (1992). Mechanisms underlying abnormal trafficking of malignant progenitors in chronic myelogenous leukemia. Decreased adhesion to stroma and fibronectin but increased adhesion to the basement membrane components laminin and collagen type IV. J. Clin. Invest. *90*, 1232–1241.

Verfaillie, C.M., Hurley, R., Zhao, R.C., et al. (1997). Pathophysiology of CML: do defects in integrin function contribute to the premature circulation and massive expansion of the BCR/ABL positive clone? J. Lab. Clin. Med. *129*, 584–591.

Voulgari, A., and Pintzas, A. (2009). Epithelial-mesenchymal transition in cancer metastasis: mechanisms, markers and strategies to overcome drug resistance in the clinic. Biochim. Biophys. Acta *1796*, 75–90.

Wang, Z., Li, Y., Ahmad, A., et al. (2011). Pancreatic cancer: understanding and overcoming chemoresistance. Nat. Rev. Gastroenterol. Hepatol. *8*, 27–33.

Woodring, P.J., Litwack, E.D., O'Leary, D.D., et al. (2002). Modulation of the F-actin cytoskeleton by c-Abl tyrosine kinase in cell spreading and neurite extension. J. Cell Biol. *156*, 879–892.